Parsing medial prefrontal cortex: A joint meta-analytic and graph-theoretic approach.

Claudio A. Toro-Serey[a,1,2] **and Joseph T. McGuire**[a,1]

[a]Boston University, Department of Psychological and Brain Sciences, 64 Commonwealth Ave., Boston, 02250

This manuscript was compiled on August 15, 2018

(Current count: 153) Valuation effects are consistently observed in medial prefrontal and posterior cingulate cortex (mPFC and PCC). The spatial extent of these effects is mostly indistinguishable from the default mode network (DMN) in existing meta-analyses. However, little is known about how valuation effects fit within the broader functional architecture of mPFC and PCC, or whether that architecture is consistent or idiosyncratic across individuals. Here we complement a meta-analysis with fMRI-based graph theoretic approaches to subdivide mPFC and PCC at the single-subject level. Our results suggest the functional topography of mPFC has substantial variability across individuals. This highlights the potential usefulness of estimating brain effects at the individual level in this region, and points to limitations of aggregative methods such as coordinate-based meta-analysis in determining whether valuation and DMN effects emerge from common or separable brain systems. Our approach shows promise in addressing this issue through future manipulations of valuation.

Networks | DMN | Valuation

(current, 676 words. Aim for 650)

The medial prefrontal cortex (mPFC) has been suggested to subserve many of the cognitive abilities that differentiate humans from other animals (Barbas & Garcia-Cabezas, 2016). Specifically, this region has been related to decision making (Bartra, McGuire, & Kable, 2013), memory encoding (Shacter, Addis, & Buckner, 2007), and default mode deactivation (DMN) (Yeo et al., 2011), among ohters. While much has been discovered about this area in primates (Barbas & Garcia-Cabezas, 2016), the lack of direct measurements of neuronal activity makes this a tough area to record in humans, one that nowadays relies mostly on functional MRI (fMRI). Unfortunately, the mPFC is especially challenging to image, as the oxygen-related signal recorded by fMRI is contaminated by the oxygen in the sinuses (Logothetis, 2008). In addition, this area is subject to more idiosyncratic cortical folding than any other region (Zilles, Palomero- Gallagher, & Amunts, 2013), thus adding a level of complexity to the generalizable dissection of topographic functional roles within mPFC.

Previous meta analytic studies have provided important insights on the psychological phenomena attributed to mPFC subregions. For example, de la Vega et al. (2016) found subdivisions of mPFC and MCC that are significantly tied to decision making in the literature. In particular, they show that more ventral regions are more tightly associated with reward and fear. However, this pattern overlaps with their finding that vmPFC also coactivates with DMN regions, and find no topographical distinction between these phenomena. Similarly, the results from Bartra et al and Laird et al show that this region can't be subdivided into DMN vs subjective value (acikalin, chris, russ). However, meta analyses rely on peaks often derived from group-averaged data. Recent work has prescribed relevance to the analysis of single subjects in fMRI. Yeo et al (2018) propose the use of individualized topologies when identifying functional networks. Gordon et al identify important idiosincrasies in oversampled subjects. Similarly, Braga and Buckner show that finer subdivisions of the DMN are possible when looking at each subject independently. This opens up the possibility that distinctions between DMN and subjective value are possible at this finer level of resolution, but would otherwise be masked in meta analytic work.

Braga & Buckner's work is particularly informative when it comes to subdividing DMN. However, the seed-based functional connectivity analysis is sensitive to the selection of the seed. A natural next step would be to recruit all possible patterns of covariation within this network. A popular alternative is to rely on graph theoretic methods, which provide a characterization of networks that organically fits brain dynamics (provides an organic avenue to understand brain dynamics?), and thus permits the consideration of the full covariance structure of brain networks. (ADV & Tal somewhere here).

Given the shortcomings of study-specific and cross-study analyses mentioned above, there is potential value in combining complementary strengths from both approaches. Focusing on resting state data has been successful in determining a number of neural phenomena, including disentangling auditory and visual attention areas (Tobyne, Osher, Michalka, & Somers, 2017).

One great advantage of network science is the ability to characterize connectivity in a way that allows for comparisons among individuals in a meaningful way (Garcia, Ashourvan, Muldoon, Vettel, & Bassett, 2018), thus letting us address the idiosyncrasies mentioned above. In this study, we aim to subdivide mPFC into subject-specific DMN and non-DMN areas, so that we can generate more informed topographic targets for future studies of decision making. We address this aim at 3 levels of granularity: 1) across the literature

Significance Statement

Authors must submit a 120-word maximum statement about the significance of their research paper written at a level understandable to an undergraduate educated scientist outside their field of speciality. The primary goal of the Significance Statement is to explain the relevance of the work in broad context to a broad readership. The Significance Statement appears in the paper itself and is required for all research papers.

Please provide details of author contributions here.

Please declare any conflict of interest here.

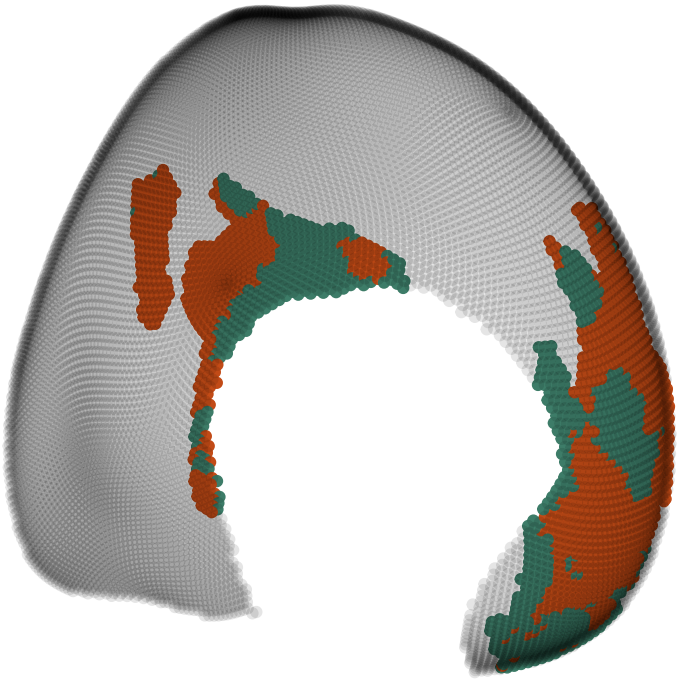

Fig. 1. Template brain.

(meta-analysis), selecting a number of regions of interest (ROI) that show significant overlap and specificity between DMN and decision making; 2) full-brain connectivity of actual fMRI data, using a pre-specified brain atlas; and 3) characterizing the connectivity of surface vertices (small units of function that contain oxygen-dependent neural information across time) for the regions selected in step one. I performed the last two steps at an individual subject level for 3 subjects, hoping to find some commonalities among them. In this way, I attempted to extract functional topographical information from topological network features.

Results

Discussion

(1500 words max)

Methods

See http://www.jneurosci.org/content/preparing-manuscript

Meta-analysis To perform the first step, I used data from a metanalysis that gathered peak brain coordinates of activity from studies of valuation (n = 27 studies) and DMN (n = 77). These are the surviving areas post-statistical thresholding from each study. I analyzed this data by mapping the peak cortical coordinates to an atlas of the human cortical surface (Glasser et al., 2016). This produced a list of standardized parcels that were reported on each study. The advantage of utilizing this atlas was threefold: first, it reduced the number of functional vertices from 60,000 (cortical surface vertices) to 360 (cortical parcels). Second, it standardizes the vertices from the first to the second stage of my study. Finally, it allowed me to project each area on a brain space without much clutter. Since each vertex is embedded with topographical information, and since functional topography is essential to my question, I mostly project my results onto brain space.

I thus generated two undirected, loop-less, weighted graphs in which each vertex was a brain parcel, and edges correspond to the number of times each pair of them co-occurred across studies. Since different decision tasks use different sensory modalities, and since sensory areas get sometimes reported as unrelated peak coordinates in DMN studies, I bootstrapped the co- occurrences across studies and removed edges whose co-occurrences lied below the 90th percentile. Based on this, only edges with co-occurrences higher than 8 were preserved, and the remaining unconnected vertices (brain regions) were discarded. With these graphs set up, I computed the strength and betweenness centrality in order to capture each parcel's centrality in the valuation and DMN literatures separately.

In order to select of regions of interest (ROI) from mPFC and other brain areas that are central to valuation and DMN literatures, I first bootstrapped the mean strength for each graph separately, and chose areas with strength above the 95th percentile of this distribution. Next, I took the intersection of these areas, such that the final ROIs were brain regions that overlapped between DMN and valuation in the literature (and thus my main target for dissociation).

Whole Brain Parcellated connectivity For the second step, in order to actually quantify the intrinsic connectivity of these ROIs in the brain, I used data from the Human Connectome Project. Specifically, I acquired resting-state fMRI activity from 3 subjects, all of whom have been preprocessed according to industry standards to allow for group-level comparisons (Tobyne et al., 2017). Each data set contained around 1 hour of signals represented as 4800 time points, and each subject contained 60,000 vertices. I parcellated each subject's brain according to the atlas mentioned above, so that each parcel contained the mean time series from its vertices, and correlated the mean time series among all parcels (Pearson). This produced a weighted adjacency matrix for each subject, where each of the 360 parcels is a vertex, and edges the correlations among all of them. Next, I took the exponential of the correlations, Fisher transformed them (i.e. tanh) so that all weights were positive while maintaining the shape of the original correlation distribution, and retained the edges whose adjusted p-values remained significant (FDR < 0.05). Again, I quantified each parcel's strength and betweenness, averaged them across subjects, and examined whether any of the ROIs showed uniquely high centralities. For this, I performed a permutation comparing the mean strength between the ROIs and the rest of the brain for each participant.

For the main goal of this section, I maximized the strength-based modularity metric as a community detection method (fast-greedy algorithm), so that I could check if all the DMN ROIs from the previous section were affiliated with the same community. While this measure has resolution problems at large and low scales (Fortunato & Hric, 2016), if it does extract a close match to standard DMN networks, it could act as a good method for the final stage of the project (but see Peel, Larremore, and Clauset 2017 for issues with ground-truth). Even though this analysis is mainly geared to confirm that these ROIs are jointly captured, this step also let me examine whether some of the ROIs could be subdivided into DMN and non-DMN regions at this level of granularity.

In order to evaluate the validity of the modularity-based communities, I also clustered the brain by means of spectral partitioning. Specifically, I took the Fiedler vector (eigenvector

associated with the second lowest eigenvalue) from each participant's normalized Laplacian matrix, and divided the brain by the sign of the eigenvector values. This analysis served the additional purpose of more strictly dividing the brain into DMN and non-DMN communities. Importantly, given the high density of these networks (see results), spectral partitioning was unlikely to face the issues associated with its use in sparse networks (Fortunato & Hric, 2016). Finally, to quantify the agreement of these community methods, I computed both the adjusted rand index and variation of information distance (normalized by the logarithm of the number of vertices, 360 in this case) between them per subject. The adjusted rand index denotes the proportion of vertices that coincide in affiliation across partitions, and compares this score to a baseline given by the expectation based on a random vertex assignment for an equal number of clusters across partitions. On the other hand, variation of information gives a general sense of the amount of information to be gained by the complementary community partitioning (Meila, 2007), measured by the addition of the conditional entropies per combination of clusters across partitions. While the rand index is more easily interpreted, it suffers from the assumption that the baseline should have an equal number of vertices per cluster across partitions, which is not necessarily the case. Therefore, I used variation of information as a more robust similarity metric (Fortunato & Hric, 2016). Importantly, due to having just 3 subjects, I abstained from performing formal statistics on the descriptive measures that I show.

Within-ROI Connectivity For the third stage, I "zoomed in" each subject's brain by computing the correlation among all of the surface-vertices contained within each ROI across all the ROIs, and applied the same correction as in step two. That means that the vertices became smaller functional brain units that are connected by the same type of edge (i.e. adjusted correlations) as in step two. This time, I only focused on partitioning the brain through modularity and spectral partitioning to see if the ROIs can be subdivided at this finer level of resolution. It is worth noting that while communities across subjects should be similar, the idiosyncrasies explained previously (i.e. cortical folding) should produce noticeable differences as well.

This time I added two new areas to the ROIs: 7m, as this area had unique relevance in DMN when compared to valuation (evidenced by its connectivity strength in DMN and chi-squared permutation in the meta-analysis, see results), and V1, as this visual processing area should not be affiliated with DMN. These regions thus acted as dual reference points, such that the community affiliated with 7m should denote DMN, while V1 indicated non-DMN. As before, I tested the validity of the partitions using the adjusted rand index and normalized variation of information. However, this time I also used the rand index to quantify the community correspondence between subjects. Specifically, I divided each subject's spectrally-partitioned brain into PCC and mPFC topographical zones (posterior and frontal brain, respectively), and computed the index of each region between subjects. The high cross-subject heterogeneity of cortical folding of mPFC should produce relatively low rand indices, while the more homogeneous PCC should display the opposite pattern. This analysis was meant to tackle the subject-specific limitations discussed above. The final patterns were inspected visually.

References

Figures and Tables should be labelled and referenced in the standard way using the `\label{}` and `\ref{}` commands.

Figure

$$fig : frog$$

shows an example of how to insert a column-wide figure. To insert a figure wider than one column, please use the `\begin{figure*}...\end{figure*}` environment. Figures wider than one column should be sized to 11.4 cm or 17.8 cm wide.

Single column equations. Authors may use 1- or 2-column equations in their article, according to their preference.

To allow an equation to span both columns, options are to use the `\begin{figure*}...\end{figure*}` environment mentioned above for figures, or to use the `\begin{widetext}...\end{widetext}` environment as shown in equation

$$eqn : example$$

below.

Please note that this option may run into problems with floats and footnotes, as mentioned in the cuted package documentation. In the case of problems with footnotes, it may be possible to correct the situation using commands `\footnotemark` and `\footnotetext`.

$$\begin{aligned}(x+y)^3 &= (x+y)(x+y)^2 \\ &= (x+y)(x^2+2xy+y^2) \\ &= x^3+3x^2y+3xy^3+x^3.\end{aligned}$$

Supporting Information (SI). The main text of the paper must stand on its own without the SI. Refer to SI in the manuscript at an appropriate point in the text. Number supporting figures and tables starting with S1, S2, etc. Authors are limited to no more than 10 SI files, not including movie files. Authors who place detailed materials and methods in SI must provide sufficient detail in the main text methods to enable a reader to follow the logic of the procedures and results and also must reference the online methods. If a paper is fundamentally a study of a new method or technique, then the methods must be described completely in the main text. Because PNAS edits SI and composes it into a single PDF, authors must provide the following file formats only.

SI Text. Supply Word, RTF, or LaTeX files (LaTeX files must be accompanied by a PDF with the same file name for visual reference).

SI Figures. Provide a brief legend for each supporting figure after the supporting text. Provide figure images in TIFF, EPS, high-resolution PDF, JPEG, or GIF format; figures may not be embedded in manuscript text. When saving TIFF files, use only LZW compression; do not use JPEG compression. Do not save figure numbers, legends, or author names as part of the image. Composite figures must be pre-assembled.

3D Figures. Supply a composable U3D or PRC file so that it may be edited and composed. Authors may submit a PDF file but please note it will be published in raw format and will not be edited or composed.